PDF Estimation and Liquid Water Content Based Attenuation Modeling for Fog in Terrestrial FSO Links

Sajid SHEIKH MUHAMMAD[1], *Muhammad SALEEM AWAN*[2], *Abdul REHMAN*[1]

[1]Dept. of Electrical Engineering, National University of Computer and Emerging Sciences (FAST-NU), Lahore, Pakistan
[2]Institute for Broadband Communication, Graz University of Technology, Inffeldgasse 12, A-8010 Graz, Austria

sm.sajid@nu.edu.pk, m.saleemawan@student.tugraz.at, abdulrehman.rana@hotmail.com

Abstract. *Terrestrial Free-space optical communication (FSO) links have yet to achieve a mass market success due to the ever elusive 99.999% availability requirement. The terrestrial FSO links are heavily affected by atmospheric fog. To design systems which can achieve high availability and reliability in the presence of fog, accurate and better models of fog attenuation need to be developed. The current article puts forth appropriate probability density function estimates for received signal strength (hereafter RSS) under fog conditions, where variations in the RSS during foggy events have been statistically characterized. Moreover, from the surface observations of fog density, liquid water content (hereafter LWC) of fog is estimated. The actual measured optical attenuations are then compared with the optical attenuations estimated from LWC. The results presented suggest that fog density measurements carried out are accurate representation of the fog intensity and the attenuation predictions obtained by the LWC estimate match the actual measured optical attenuations. This suggests that the LWC is a useful parameter besides visibility range to predict optical attenuations in the presence of hydrometeors.*

Keywords

Free-Space Optics (FSO), Fog Modeling, Probability Density Function (PDF), Liquid Water Content (LWC), Drop Size Distribution (DSD).

1. Introduction

FSO links are of prime importance in order to fulfill ever growing demands of data rates for future terrestrial and ground-space communication applications. With the growing demand for high bandwidth data rate access, many competing technologies have evolved in an effort to solve the last mile bottleneck problem within metropolitan area networks [1]. FSO promises a very high bandwidth associated to the optical frequencies without the need of digging up the ground for laying the fiber. FSO links have notable advantages over both radio frequency (RF) and fiber optics due to the absence of channel dispersion and nonlinearities. However, the main reasons for the relatively slow acceptability of FSO as a preferred access technology, are the atmospheric attenuators that significantly degrade the link performance [2]. In recent years, many different solutions, like coded modulation techniques, adaptive optics, and employing quantum cascade laser (QCL) with emission wavelengths in the infrared range have been proposed for better performance of FSO under different atmospheric influences [2], [3], [4], [5]. However, most researchers proposed improvements in FSO system design by concentrating only on the turbulence induced fading issues and have extensively utilized the models developed for weak and strong turbulence in the channel to get insight into the system design aspects [3], [4], [6], [7]. While much less attention has been paid to the other FSO link attenuators like fog, snow and clouds. Recent studies concluded that optical power losses for dense maritime fog and moderate continental fog conditions are up to 480 dB/km and 120 dB/km, respectively [8], [9], [10]. Intense shower and heavy snowfall conditions result in optical signal attenuations approaching 30 dB/km and 70 dB/km, respectively [11]. Empirical models e.g., the Crane and ITU-R model have been proposed in literature for rain and snow attenuations [11], [12], [13], while the well known Kim and Kruse models are extensively utilized for empirical modeling of fog environments [14], [15].

The fog modeling efforts have remained concentrated till now on the development and improvement of empirical models to get estimates of the attenuation caused by fog [14], [15], whereas the turbulence modeling effort always concentrated and worked towards attaining and improving upon tractable probability density functions for the irradiance fluctuations [16], [17], [18]. Not many attempts in this direction have been made for the fog case. The prime reason is the behavior of fog formation, its long persistence in the atmosphere and the fact, that many times a fog causes such high attenuations that would render the link unavailable [10]. The empirical models provide good estimates of attenuations caused by the atmospheric link impairments; however, they provide no insight about the RSS variations. FSO system designers have been in the need of stochastic models so that they might get insight into the RSS variations under the influence of the atmospheric attenuators. The stochastic models can provide the basis for appropriate system design enhancements like well suited modulation schemes, channel codes, equalizers and estimators for the terrestrial FSO link. Proposing system design enhancements which improve the performance only under turbulent conditions is not enough.

Fog modeling is the focus of this article, and Section 2 provides novel results on PDF estimation of RSS during a foggy event, whereas Section 3 introduces a new technique of employing LWC to predict visibility range and the corresponding fog attenuations. Section 4 concludes the article by highlighting the significance of these advancements in fog modeling for terrestrial FSO links.

2. PDF Estimation of RSS for Continental Fog Conditions

A novel approach of achieving a tractable probability density function of the received signal strength under fog attenuation has been investigated. The continental fog has characteristics which allow us to model the received signal strength by standard curve fitting techniques. We provide below the results achieved through analysis of data acquired through measurement campaigns at the continental city of Graz [20]. A fog event measured in Graz, Austria on January 31, 2006 has been analyzed. The RSS of the transmitted optical signals having 850 nm and 950 nm wavelengths, over a link distance of approximately 800 m, were recorded by a unidirectional FSO link. Fig. 1a)–d) shows the distribution of the received power (dBm) for the complete fog event that spanned around 14 hours, for 1 hour, for one minute and for 30 seconds, respectively.

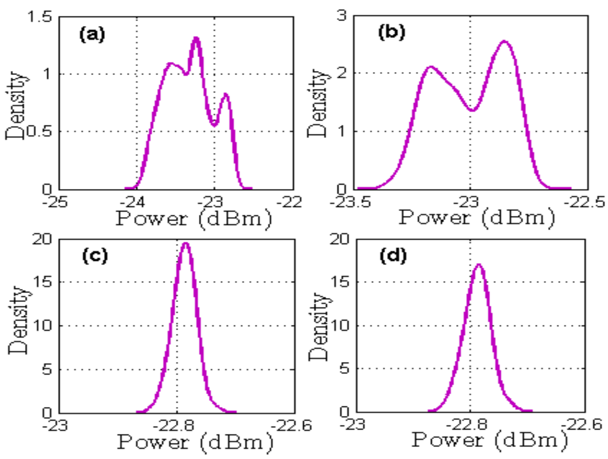

Fig. 1. Received power distribution of a selected fog event recorded in Graz on 31.01.2006 for different time durations

.

These plots are drawn using *Kernel smoothing density estimate* i.e., `[f,xi] = ksdensity(x)` function in MATLAB. This function computes a probability density estimate of the sample in some vector x, while f is the vector of density values evaluated at the points in xi. The density estimate is based on a normal kernel function and the density is evaluated at 100 equally spaced points that cover the range of the data in x [21]. The distribution clearly exhibits a multimodal PDF with a spread of 1 dBm. The constituent parameters of fog including the drop size distribution undergoes significant changes over large spans of time resulting in the mean of the distribution of attenuation shifting to different values and thus creating a multimodal probability density function. To analyze the distribution of the RSS on hourly scale, we provide the PDF of received power for this selected fog event as shown in Fig. 1b). As clearly evident, the PDF has a bimodal shape with two distinct modes around -23.2 dBm and -22.8 dBm of the received power. Forfurther analysis, the PDFs have been drawn on a minute and 30-second scales (as shown in Figs. 1c) and 1d)), respectively. It is quite interesting to note that the PDFs now take the shape of a standard Gaussian curve once the time span is reduced to a minute or less.

To further investigate the trend of RSS in continental fog, we analyze another continental fog event that is also recorded in Graz on November 18-19, 2009. The total duration of this fog event was about 13 hours (started around 5 PM on Nov. 18, 2009 and lasted until 8 AM on Nov. 19, 2009). The optical attenuations recorded a maximum value of 140 dB/km averaged on a minute scale. The received power distribution for this selected whole fog event is given in Fig. 2a). This is followed by received power distributions on 1 hour, 10 minute, 1 minute, and 30-second time intervals as shown in Figs. 2b), 2c), 2d), and 2e), respectively.

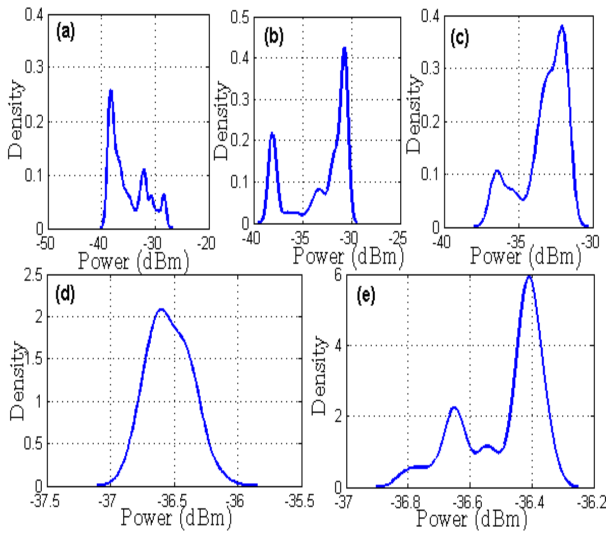

Fig. 2. Received power distribution of a selected fog event recorded in Graz on 18-19.11.2009 for different time durations.

It is clearly evident that multimodal behavior is observed for longer time intervals (on hourly basis). As we move down to shorter time intervals, the curves depict a trend towards Gaussian distribution. The slight differences observed in terms of the details of the PDF's shape acquired by the RSS in the two events (Figs. 1 and 2) can be attributed to the fog characteristics of the particular event. The overall trend is that of multimodal distribution over large time scales (see Figs. 1b) and 2b)) and a trend towards Gaussian or a skewed Gaussian PDF when measured on smaller time intervals in both the representative fog events. The results analyzed over smaller time intervals are more significant as they can then be suggestive towards signal estimation, selection of forward error correction codes and thus an improved FSO system design.

For further statistical analysis of the fog attenuations, the statistical parametric values for the two fog events are summarized in Tab. 1. The variance of continental fog data recorded a sharp decrease when measured at reduced time scales. At smaller time intervals like 1 minute and 30 seconds, the variance became really small depicting that the attenuation almost becomes stable. This sharp decrease in variance on smaller time intervals suggests a rather stable characteristic of the continental fog as compared to other fog types like maritime (advection) fog. In other words, it means that the continental fog retains its attenuation characteristic once it sets in. It shall be noted that the link distance was about 800 m for the winter 2006 fog event, and about 80 m for winter 2009 fog event.

The comparison of Skewness reveals interesting insight in the fog attenuation analysis. The received power for winter 2006 interval has Skewness approaching zero for shorter intervals (1 hour and lesser). However, for larger time intervals (> 3 hours) the curve is skewed to the right; indicating that the signals with lesser power are received more frequently than higher powered signals. A similar trend is observed for the winter 2009 fog event. The high kurtosis and small variance signifies a stable link. Higher variance alongside high kurtosis would depict infrequent extreme deviations in the received power. The generic trend in the data analyzed is a higher kurtosis than for Gaussian distribution.

Probability density function fitting has been tried to the PDF estimates of the complete fog events recorded and the results have been summarized in Tab. 2. The sum of the square error (hereafter SSE) difference at each of these curves with the original nonparametric density estimates was evaluated and clearly the best fit shall have the smallest number of squared errors. The lognormal PDF has been found to be the closest fit for the continental Graz fog event of 2006, and Gamma PDF for Graz 2009 fog event. However, as evident from the complete fog event's real PDFs (Figs. 1a) and 2a)), it can be concluded that the attempts to find the best fit do not really reveal the true picture.

3. Methodology of Estimating Fog Attenuations from LWC

Fog that is characterized by several physical parameters such as particle size distribution, temperature, humidity and LWC has been extensively modeled by drop size distribution and visibility range. In this part of the paper an innovative approach of fog attenuation prediction based on LWC is given. This section comprises of methodology for fog attenuation using LWC in subsection 4.1, after that different empirical models based on visibility range estimate from LWC are elaborated in 4.2, followed by analysis of simulation results and comparison with actual measured FSO attenuation in subsection 4.3.

3.1 Relationship between Fog's Drop Size Distribution and LWC

The size distribution of the fog droplets is usually described by modified gamma drop size distribution (MGDSD) as given by

$$C(r) = N_0 r^m exp(-\Lambda r^{\sigma})\Delta r, \qquad 0 \leq r \leq \infty \tag{1}$$

where r is the particle radius. N_0, m, Λ and σ are parameters which characterize the particle size distribution. Fog is usually characterized by N_0, m and Λ with $\sigma = 1$ [22]. For dense fog these parameter values are 0.027, 3 and 0.3 respectively and for moderate continental fog the values are 607.5, 6 and 3. If N_d is the actual total concentration of the fog droplets per cubic centimeter of air then the real profile of the fog droplets is given by multiplying C(r) by N_d [23]. Therefore, following (1) the LWC in g/m^3 is defined as

$$LWC = \rho_w N_d \frac{4}{3} \int_0^\infty \pi r^3 C(r) dr \tag{2}$$

where ρ_w is density of water in g/cm^3. The values of LWC resulting from (2) and the corresponding set of MGDSD parameters giving the best fit curves relative to eight size spectra of small water droplets for a visibility range of 1 km are given by Claudio Tomasi et. al [23]. Given the third power radius in(2), it is suggested that water droplets smaller than 3 μm have a very small contribution towards LWC and, therefore, could be neglected [24]. The effective droplet radius (r_e) in terms of DSD is given by (3) below.

$$r_e = \frac{\int_0^\infty r^3 C(r) dr}{\int_0^\infty r^2 C(r) dr} = 30000 \frac{LWC}{PSA}. \tag{3}$$

It is important to mention that r_e is the radius of the fog particles of *single diameter droplet* having the same LWC, and particle surface area (hereafter PSA) measured in (cm^2/m^3). LWC and PSA are both important parameters to estimate fog attenuations caused by scattering of fog particles. When fog particles are assumed spherical in shape, then PSA is given by,

$$PSA = 10^{-2} \cdot 4\pi \int_0^\infty r^2 C(r) dr. \tag{4}$$

PSA and LWC of fog and clouds droplet size distribution can be estimated from MGDSD, i.e. $C(r)$. Assuming modified gamma drop size distribution MGDSD (as given by (1)), and provided m is specified, N_0 and Λ are given by

$$N_0 = \frac{3 \cdot 10^6 (LWC \cdot \Lambda^{m+4})}{4\pi\Gamma(m+4)}, \tag{5}$$

$$\Lambda = \frac{(m+3)}{r_e}. \tag{6}$$

Fog event dated 31.01.06						Fog event dated 18-19.11.09					
Duration	**Mean**	**Variance**	**Range**	**Skewness**	**kurtosis**	**Duration**	**Mean**	**Variance**	**Range**	**Skewness**	**kurtosis**
14 hours	-26.578	6.3662	6.3662	0.0148	1.3356	**16.5 hours**	-35.1410	10.7702	11.4670	0.6593	2.1170
1 hour	-23.0037	0.0236	0.6520	-0.141	1.6875	**1 hour**	-33.2381	8.7600	7.8820	-0.7646	1.9026
10 minutes	-22.8052	0.0006	0.1680	-0.0561	2.8762	**10 minutes**	-33.2881	2.3010	5.3510	-1.0226	2.8677
1 minute	-22.7874	0.0003	0.0930	-0.0919	3.5764	**1 minute**	-36.5382	0.0233	0.6610	0.2697	2.4208
30 seconds	-22.7876	0.0004	0.0930	0.038	3.3312	**30 seconds**	-36.4930	0.0166	0.4550	-0.8895	2.4994

Tab. 1. Statistical parameter values (dB) of two representative fog events recorded in Graz.

Density functions	Fog event dated 31.01.06				Fog event dated 18-19.11.09			
	Mean	**Variance**	**Distr. parameters**	**SSE**	**Mean**	**Variance**	**Distr. parameters**	**SSE**
Lognormal	-26.5784	6.46165	μ=-3.27555, σ=0.095423	0.6212	-34.1332	17.2807	μ=-3.52291, σ=0.12134	0.2796
Gamma	-26.578	6.40128	a=110.351, b=0.240849	0.6217	-34.1273	16.7069	a=69.7118, b=0.489548	0.2733
Exponential	-26.578	706.391	None	1.2388	-34.1273	1164.67	None	0.5367

Tab. 2. Statistics of three best fit density functions of two representative fog events in Graz.

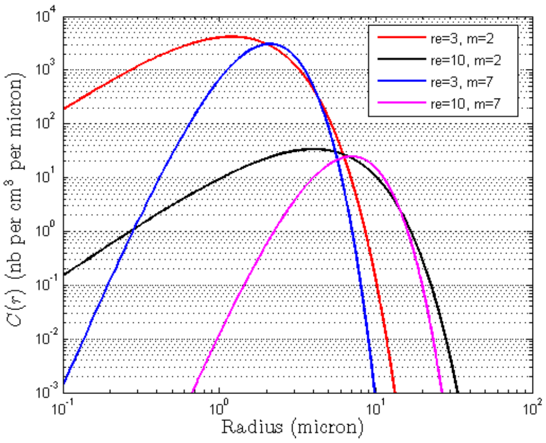

Fig. 3. The MGDSD of fog for different DSD parameter values against LWC=0.5 g/m^3.

Here $\Gamma()$ is the gamma function. Fig. 3 illustrates the influence of three DSD parameters of the modified gamma distribution for a given value of LWC = 0.5 g/m^3.

LWC varies significantly depending on the type of fog or cloud present in the atmosphere at a particular location. Their classification is highly related to the amount of LWC as well as to their origin. The combination of LWC and the origin allows to readily predict the types of conditions that will be most likely in the vicinity of the free-space optical link. Fog, having very low densities, contains very small amount of water and thus results in lower values of LWC around 0.05 g/m^3 for a moderate fog (visibility range around 300 m). Much higher values of LWC (around 0.5 g/m^3) usually mean formation of thick or dense fog (visibility range of about 50 m) [20]. Similarly, clouds may have LWC value of 0.06405 g/m^3 and 1-3 g/m^3 for Cirrus and Cumulonimbus clouds, respectively measured in the same amount of space [22]. Fog or cloud droplets of the maritime origin tend to have fewer water droplets having relatively larger size radius than the continental droplet size [22], [25]. The concentration of maritime origin droplets lies between 100 drops/cm^3 to about 200 drops/cm^3, whereas the concentration of continental origin droplets is about 900 drops/cm^3 [26].

3.2 Models Relating LWC to Visibility Range

Many models exist that relate DSD of fog or clouds to the optical attenuations for the FSO links. Due to the complexity of computing the DSD of fog or clouds at a particular location, models that relate visibility range to the optical attenuations have been developed. It may not be straightforward to compute the visibility range because of availability of transmissiometer systems and their high installation costs involved. Hence, there is a need to find an alternative solution to predict visibility range from some microphysical properties of certain atmospheric conditions like fog, rain, snow and clouds. LWC seems a suitable option as it is easily computable and, moreover, existing empirical models could then be used that relate visibility range to the LWC.

The variability in the fog microstructure causes a considerable variability in the reduction of visibility range induced by the presence of small water droplets in the air. Numerous researchers have aimed at defining relationships between associated visibility range reduction and the overall characteristics of fog. Most of them have focused on the power law relationship between fog's LWC and its associated extinction coefficient [23], [27]. The general form of LWC and visibility range relationship derived from the ample set of data related to fog's evolutionary stages is given by

$$V = b(LWC)^{-2/3} \tag{7}$$

where V is the visibility range and LWC is the amount of Liquid Water Content (g/m^3). Parameter b takes on specific values for different fog conditions as shown in Tab. 3.

Another relationship dealing with LWC and the corresponding optical extinctions is given by

$$\beta_{ext} = p(LWC)^a. \tag{8}$$

Here, β_{ext} is the optical extinction coefficient. The proportionality constant p is related to specific fog conditions. Experimental results show considerable variability, with values falling in the range of $65 \leq p \leq 178$ and $0.63 \leq a \leq 0.96$ [28]. A relationship for visibility range as a function of both LWC and the droplet size was proposed by J. E. Jiusto

Fog Type	b	Reference
Dense Haze	0.013	Claudio Tomasi et. al
Continental fog (dry and cold)	0.034	Claudio Tomasi et. al
Maritime fog (wet and warm)	0.060	Claudio Tomasi et. al
Dense Haze and Selective fog	0.017	Eldridge et. al
Stable and evolving fog	0.024	Eldridge et. al
Advection fog	0.02381	Koester and Kosowsky

Tab. 3. Fog types and the values of coefficient b to estimate visibility range from LWC.

who showed that LWC is directly related to droplet size [29]. More recently Gultepe et al. proposed a relationship between visibility range V and the product of droplet number concentration N_d and LWC [30] as given by Equation 9. This model recognizes the presence of variability in fog droplet sizes and their role in optical extinctions in different fog conditions by influencing the visibility range parameter

$$V = 1.002(LWC \cdot N_d)^{-0.6473}. \tag{9}$$

The maximum value for N_d and LWC used in derivation of (9) are about 400 cm^{-3} and 0.5 g/m^3, respectively, whereas the minimum values are 1.0 cm^{-3} and 0.005 g/m^3, respectively. This model recognizes the presence of variability in droplet sizes and their contribution towards reduction of visibility range in fog. Under a project named Fog Remote Sensing and Modeling (FRAM), a model has been developed from the empirical data to characterize different phases of maritime fog (e.g., formation, evolution and dissipation) that deals with marine fog and is given by [31]

$$V = 0.856(LWC \cdot N_d)^{-0.609}. \tag{10}$$

(10) suggests that when LWC is fixed, N_d should decrease to obtain large visibility range values, e.g. during fog dissipation phase. In case of small droplets evaporation, some large droplets tend to be formed such that when these large droplets reach a critical size (diameter > 20 μmm) they drizzle out [31].

Fig. 4a)-d) shows simulation results for the visibility range for fixed values of N_d, fixed LWC, the continental and maritime fog models defined by (9) & (10), and the simulation model of (8), respectively. It is evident from this plot that visibility range decreases with increasing N_d and LWC. In Fig. 4-(c), the model labelled as maritime (advection) fog is simulated using (10), whereas models labelled as continental fog and maritime fog are simulated using (9).

Now, in order to estimate the fog's LWC (g/m^3) values directly from the fog density values (mg/m^3), the following procedure can be adopted. The fog density is measured with a simple optical device, whose output values may have big fluctuations as they are measured on the seconds time scale. So, conversion from fog density values to LWC values first requires smoothing of the data values since LWC can not change so rapidly. This can be achieved through averaging of the instantaneous values of LWC.

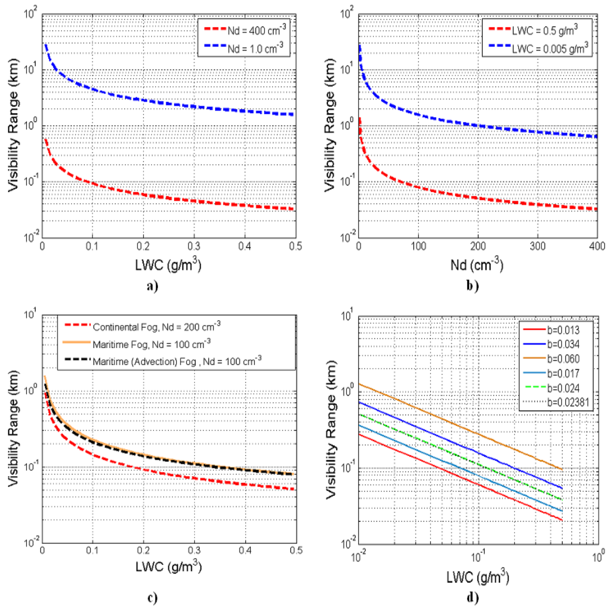

Fig. 4. Simulations of relationship between LWC, N_d and visibility range.

Let W_k be the averaged value of LWC and D_k the output of the fog sensor between 0 – 0.5 relative values, therefore their ratio is represented by a constant C given by [32]

$$C = \frac{\sum_{k=1}^{n} W_k}{\sum_{k=1}^{n} D_k} = 0.7384(g/m^3) \qquad k = 1, 2, ..., n \tag{11}$$

where n is the total number of measurement samples during the whole fog event. The momentary value of LWC in the presence of fog is thus given by

$$LWC_k = C \cdot D_k = 0.7384 \cdot D_k(g/m^3), \;\; k = 1, 2, ..., n. \tag{12}$$

The optical extinctions can be predicted from LWC values either by the power law relationship as given by (8), or by first predicting the visibility range from LWC instantaneous values using (9) & (10) for continental and maritime fog, respectively.

3.3 Results on Impact of Fog Density & LWC on the FSO Link Performance

Fig 5 shows time series of recorded fog density and LWC, temperature, relative humidity and the corresponding optical attenuations at 950 nm on a minute scale against a continental fog event recorded at Graz on November 18-19, 2009 over a 80 m FSO link. The shown values of the above mentioned parameters are from 10 AM on Nov. 18, 2009 to

10 AM on Nov. 19, 2009. The total duration of the fog event was approx. 13 hours (started around 5 PM on Nov. 18, 2009 and lasted until 8 AM on Nov. 19, 2009). The optical attenuations recorded the maximum value of 140 dB/km averaged on a minute scale. During dense fog conditions of this fog event the temperature varied around 4 – 6 °C while the relative humidity approached about 100 %. During later stage of the fog event when temperature started to increase the corresponding relative humidity decreased, and hence caused the fog to dissipate, whereas during early stage of the fog event (fog formation phase), the temperature approached 0 °C and relative humidity increased towards 100 %. Data analysis of the measured parameters reveals that maximum optical attenuation of 140 dB/km is achieved against LWC value of around 0.29 – 0.3 g/m^3 averaged over a minute scale. An average value of about 0.1198 g/m^3 for LWC was observed during the mentioned 24 hours time interval averaged over minute scales. Further analysis reveals that for a maximum value of LWC ($\sim$ 0.4 g/m^3) the corresponding value of optical attenuations is $\sim$ 130 dB/km. The possible explanation of this fact can be the variations in N_d due to sudden wind gusts, or may be due to the 1 m separation between the FSO receiver terminal and the fog sensor device. In short it is quite evident that optical attenuations are in high correlation ($\sim$ 0.6997) with the fog density variations, and the results indicate that both are strongly influenced by the severity of fog.

The plot in Fig. 6 shows the comparison between actual measured optical attenuations at 950 nm and the optical attenuations predicted from LWC momentary values. The procedure adopted to compute the predicted attenuations from LWC instantaneous values is as follows: firstly, the instantaneous values of fog density recorded by the fog sensor are converted to momentary LWC values averaged over minutes and hours time scale against the mentioned fog event using (12). Then from these momentary values of LWC, visibility range is estimated using the relationship given by (9). Once the visibility range is computed against the LWC values for the mentioned continental fog event, using Kruse and Kim model (approximations of visibility range) the corresponding specific attenuations are computed for attenuation values averaged over minutes and hours time scales for comparisons. It is important to mention that the transmission threshold was taken as 5 % while predicting the visibility range values from LWC instantaneous values. The plots given in Fig. 6a)-b) show a comparison between the measured optical attenuations and the predicted attenuations for a range of N_d against Kruse and Kim model, respectively. Different values of N_d are compared in order to get a rough idea about the fog particles concentration during certain fog event. From Figs. 6a)-b), it appears as though the particle concentration roughly varies somewhat between 100 – 250 particles/cm^3 volume as the actual measured attenuations were closer to this range of values compared to the other ranges of values. In order to get a better impression between comparisons of attenuations, plots in Fig. 6c)-d) are compared based on attenuation values averaged on a hourly time scale for both actual measured and the predicted attenuations using Kruse and Kim approximations, respectively. From these two plots, it is quite clear to observe that the particle concentration remained in the above mentioned range during this fog event. In Figs. 6e)-f), the predicted (Kruse and Kim) and actual measured optical attenuations are compared against the Cumulative Distribution Function (hereafter CDF) exceeded (%) for values averaged on a minute and hourly time scales, respectively. It is evident from these plots that the CDF of the measured and the predicted attenuations proves that the attenuation values are similarly distributed; validating the LWC estimation. Moreover, the predictions made through visibility range estimates by Kim model are quite closer to the actual measured attenuations as compared to the Kruse model. This tendency is observed because the selected fog event was a kind of dense continental type with visibility range well below 500 m most of the time. And since Kim model better describes lower visibility range conditions than Kruse, the Kim model performs better.

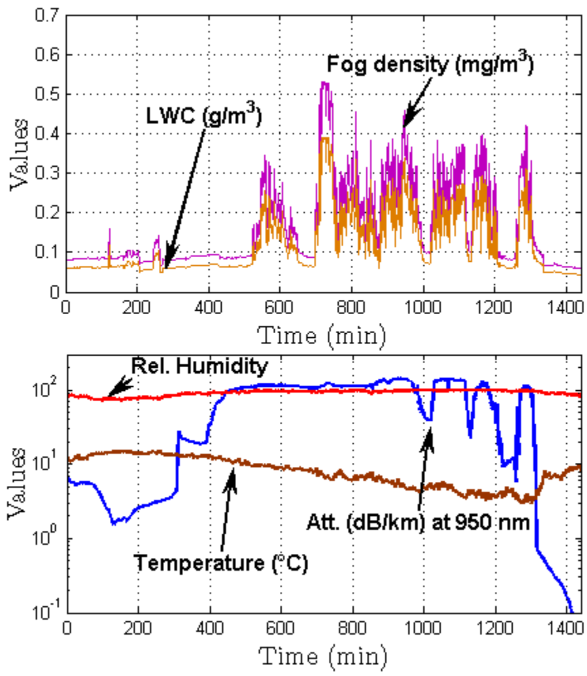

Fig. 5. Results of LWC, temperature, relative humidity and fog density variations against a continental fog event recorded in Graz.

In order to refine the precision of this technique further measurements would be required preferably for dense fog conditions in different fog environments and geographical locations. The significance of this method over prediction method based on visibility range is that this method is equally valid in order to predict attenuations for both terrestrial as well as ground-space optical links, whereas the prediction method based on visibility range is so far only applicable to horizontal FSO links.

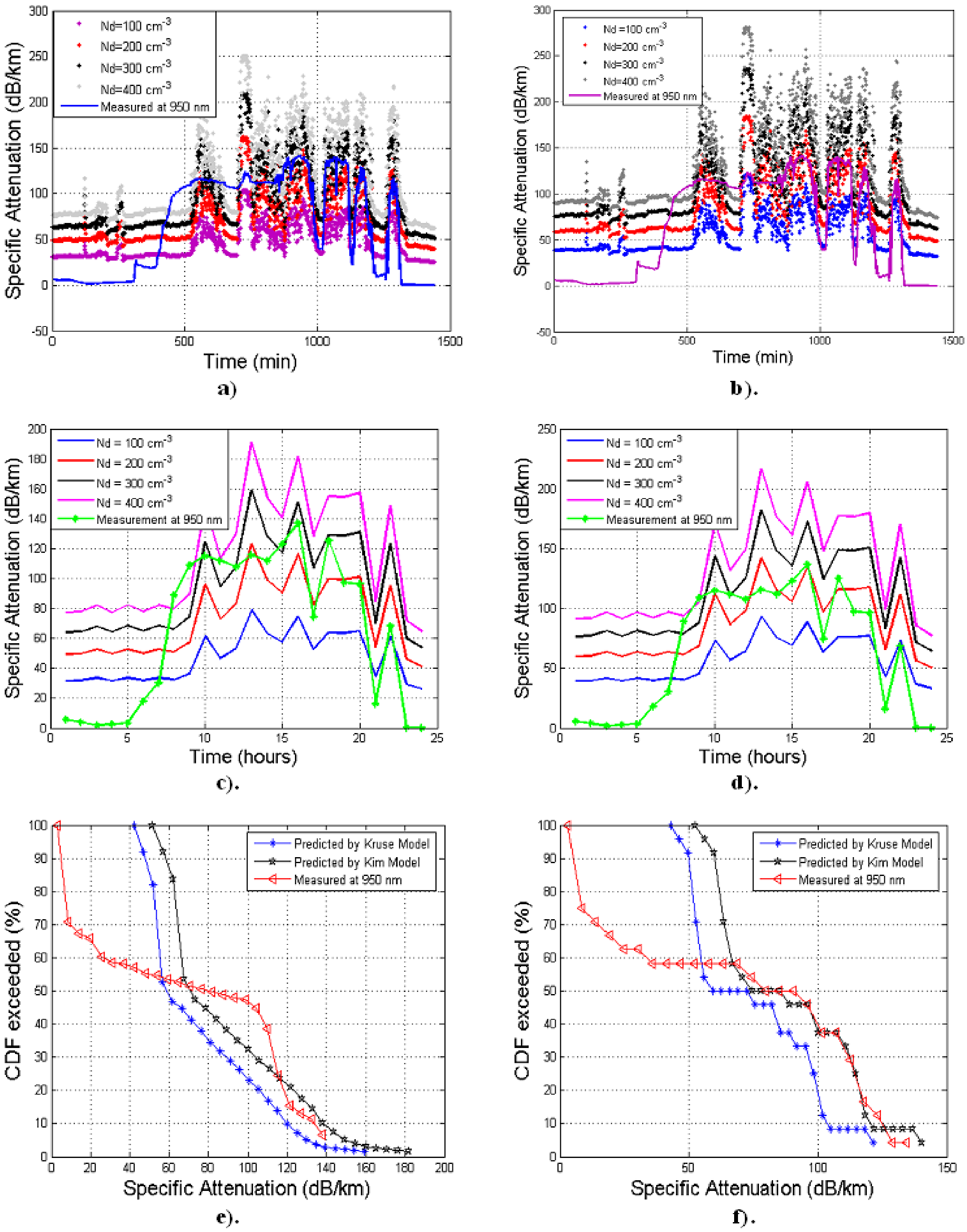

Figure 6. Comparison between measured optical attenuations from path and the predicted attenuations from momentary values of LWC; Measured attenuations and predicted attenuations by Kruse model on a minute scale (a), measured attenuations and predicted attenuations by Kim model on a minute scale (b), measured attenuations and predicted attenuations by Kruse model on a hour scale (c), measured attenuations and predicted attenuations by Kruse model on a hour scale (d), CDF (%) exceeded for measured and predicted attenuations on a minute scale (e), CDF (%) exceeded for measured and predicted attenuations on a hour scale (f).

4. Conclusions

FSO system design enhancements for terrestrial links are highly dependent upon the accuracy of the channel model utilized. Stochastic models that provide the basis for appropriate system design enhancements are a way forward as they give us the insight into the RSS variations in different fog conditions. In this article, two selected radiation fog events recorded over two different path lengths (80 m and 800 m), have been analyzed on the basis of RSS distribution and corresponding signal variations. It was noticed that smaller received power variations are observed that span around 1.5 dB for the first representative fog event over a link distance of 800 m and higher received power variations for shorter distance link (80 m) for the second event recorded in 2009. The results also showed that the RSS in the presence of a foggy channel distributed itself as a Gaussian or a skewed Gaussian PDF when measured over a small interval of time (10 minutes or shorter intervals). Further investigations on optical attenuations revealed that fog conditions are highly dependent on the amount of LWC. Through a comparison of fog density measured by a simple fog sensor device installed at the location of FSO transceivers, it was observed that fog density is in high correlation with the LWC and the corresponding optical attenuations.

A large number of fog events (a multi-year data-set with consistent state-of-the-art instrumentation) need to be analyzed in order to get statistically reliable models of drop size distribution parameters for long term predictions and also to indicate the suitability of the Gamma and Lognormal distribution functions to derive fog attenuations over the entire range of fog droplet sizes.

References

[1] DAVIS, C. C., SMOLYANINOV, I. I., MILNER, S. D. Flexible optical wireless links and networks. *IEEE Communication Magazine*, March 2003, p. 51 – 57.

[2] MAJUMDAR, A. K., RICKLIN, J. C. *Free-Space Laser Communications, Principles and Advantages*. New York: Springer Science LLC, 2008.

[3] POPOOLA, W. O., GHASSEMLOOY, Z., ALLEN, J. I. H., LEITGEB, E., GAO, S. Free-space optical communication employing subcarrier modulation and spatial diversity in atmospheric turbulence channel. *IET Optoelectronic*, 2008, vol. 2, p. 16 – 23.

[4] YAMAMOTO, H., OHTSUKI, T. Atmospheric optical subcarrier modulation systems using space-time block code. In *IEEE Global Telecommunications Conference (GLOBECOM '03), vol. 6*. New York, 2003, p. 3326 – 3330.

[5] MARTINI, R., WHITTAKER, E. A. Quantum cascade laser-based free space optical communications. *J. Optical Fiber Commun. Reports*, 2005, vol. 2, no. 4, p. 279 – 292.

[6] XU, F., KHALIGHI, M. A., BOURNNANE, S. Pulse position modulation for FSO systems: capacity and channel coding. In *Proceedings of IEEE ConTEL*. Zagreb (Croatia), 2009, p. 31 – 38.

[7] ZHU, X., KAHN, J. M. Performance bounds for coded free-space optical communications through atmospheric turbulence channels. *IEEE Transactions on Communications*, 2003, vol. 51, no. 8, p. 1233 – 1239.

[8] SHEIKH MUHAMMAD, S., FLECKER, B., LEITGEB, E., GEBHART, M. Characterization of fog attenuation for terrestrial FSO links. *Optical Engineering*, 2007, vol. 46, no. 6, p. 066001.

[9] AL-NABOULSI, M., DEFORNEL, F., SIZUN, H., SHEIKH MUHAMMAD, S. et al. Measured and predicted light attenuation in dense coastal upslope Fog at 650, 850 and 950 nm for free space optics applications. *Optical Engineering*, 2008, vol. 47, no. 3., p. 036001.

[10] GEBHART, M., LEITGEB, E., SHEIKH MUHAMMAD, S. et al. Measurement of light attenuation in dense fog conditions for optical wireless links. In*SPIE Proceedings, Optics and Photonics Symposium, vol. 5891*. San Diego (USA), 2005, p. 58910K1 – 12.

[11] NEBULONI R., CAPSONI, C. Laser attenuation by falling snow. In *Proceedings of IEEE CSNDSP 2008*. Graz (Austria), 2008, p. 265 – 269.

[12] ACHOUR, M. Simulating atmospheric free-space optical propagation: I, rainfall attenuation. *Proceedings of SPIE*, 2002, vol. 3635.

[13] SHEIKH MUHAMMAD, S., KOHLDORFER, P., LEITGEB, E. Channel modeling for terrestrial free space optical links. In *Proceedings of IEEE International Conference on Transparent Optical Networks, vol. 1*. Barcelona (Spain), 2005, p. 407 – 410.

[14] KIM, I., MCARTHUR, B., KOREVAAR, E. Comparison of laser beam propagation at 785 nm and 1550 nm in fog and haze for optical wireless communications. *Proceedings of SPIE*, 2001, vol. 214, p. 38 – 45.

[15] KRUSE, P. W. *Elements of Infrared Technology: Generation, Transmission and Detection*. New York: Wiley, 1962.

[16] AL-HABASH, M. A., ANDREWS, L. C., PHILIPS, R. L. Mathematical model for irradiance probability density function of a laser beam propagating through turbulence media. *Optical Engineering*, 2001, vol. 40, no. 8, p. 1554 – 1562.

[17] KAMALAKIS, T., SPHICOPOLOUS, T., SHEIKH MUHAMMAD, S., LEITGEB, E. Estimation of the power scintillation probability density function in free space optical links by use of multi canonical Monte Carlo sampling. *Optics Letters*, 2006, vol. 31, no. 21, p. 3077 – 3079.

[18] HILL, R. J., FREHLICH, R. G. Probability distribution of irradiance for the onset of strong scintillation. *Journal Optical Society of America*, 1997, vol. 14, p. 1530 – 1540.

[19] KOLKA, Z., WILFERT, O., KVICALA, R., FISER, O. Complex model of terrestrial FSO links. *Proceedings of SPIE*, 2007, vol. 6709, p. 67091J1 – J8.

[20] AWAN, M. S., NEBULONI, R., CAPSONI, C., CSURGAI-HARVATH, L., SHEIKH MUHAMMAD, S., NADEEM, F., KHAN, M. S., LEITGEB, E. Prediction of drop size distribution parameters for optical wireless communications through moderate continental fog. *International Journal for Satellite Communication*, 2010.

[21] *MathWorks – Matlab and Simulink for Technical Computing.* [Online] Cit. 2010-05-10. Available at: http://www.mathworks.com.

[22] SHETTLE, E. P. Models of aerosols, clouds, and precipitation for atmospheric propagation studies. *AGARD Conference Proceedings*, 1989, vol. 454, no. 15.

[23] TOMASI, C., TAMPIERI, F. Features of the proportionality coefficient in the relationship between visibility and liquid water content in haze and fog *Atmosphere*, 1976, vol. 14, no. 2, p. 61 – 76.

[24] ACHOUR, M. Simulating atmospheric free-space optical propagation: II, haze, fog and low cloud attenuations. *Proceedings of SPIE*, 2002, vol. 4873, p. 1 – 12.

[25] ITU-R P.840-3 *Attenuation due to clouds and fog. ITU-R P.840-3* Geneva (Switzerland): International Telecommunication Union, 1999.

[26] WALLACE, J. M., HOBBS, P. V. *Atmospheric Science: An Introductory Survey.* 2nd ed. London (UK): Elsevier, 2006.

[27] ELDRIGE, R. G. Mist - the transition from haze to fog. *Bull. Am. Meteorological Society Journal*, 1969, vol. 50, p. 422 – 426.

[28] GULTEPE, I., TARDIF, R., MICHAELIDES, S. C., CERMAK, J., BOTT, A., BENDIX, J., MULLER, M. D., PAGOWSKI, M., HANSEN, B., ELLROD, G., JACOBS, W., TOTH, G., COBER, S. G. Fog research: A review of past achievements and future perspectives. *Pure Applied Geophysics*, 2007, vol. 164, p. 1121 – 1159.

[29] JIUSTO, J. E. Fog structure. *HOBBS, P. V., DEEPAK. A. (Eds.) Clouds, Their Formation, Optical Properties, and Effects*. New York: Academic Press, 1981.

[30] MILLER, M. D., GULTEPE, I., BOYBEYI, Z. A new warm fog parameterization scheme for numerical weather prediction models. *Journal of Applied Meteorology*, 2006, vol. 45, p. 1469 – 1480.

[31] GULTEPE, I., ISAAC, G. A. A natural fog dissipation process in a marine fog event during FRAM. In *9th WMO Scientific Conference on Weather Modification*. Antalya (Turkey), 2007.

[32] HORWATH, L. C., BITO, J. Fog attenuation on V band terrestrial radio and a low-cost measurement setup. In *Future Network and MobileSummit 2010*. Florence (Italy), 2010. Accepted for presentation.

About Authors. . .

Sajid SHEIKH MUHAMMAD received his Bachelors, Masters and PhD in 2001, 2003 and 2007 respectively, all in Electrical Engineering. His research interests revolves around channel modeling and system design of optical wireless communications. He has published over 30 scientific articles in peer reviewed Journals and conferences, and organized the First IEEE Colloquium on Optical Wireless Communications in 2008 in Graz, Austria. He was later nominated as the guest editor for the Journal of Communication's Special Issue on Optical Wireless in 2009, and published a book entitled "Coded Modulation for Terrestrial Free Space Optical Systems" in 2010. He has been invited to the Technical review panel of major conferences and Journals publishing the latest research in the optical wireless domain.

Muhammad SALEEM AWAN received his M.Sc. from G. C. Lahore (now a University), Lahore, Pakistan in 1996. His current interests include optical wireless communication channel modeling, wireless technologies and satellite communication. He is now with the Institute of Broadband Communications, Graz University of Technology, Graz, Austria, as doctoral student since January 2007.

Abdul REHMAN graduated in BE-Telecommunication from AIOU in 2007, currently a student of MS at National University of Computer and Emerging Sciences. Working on his MS thesis he is making an effort for PDF estimation of fog's behaviour in FSO communication. His research interests are optical communication, computer networks and digital communication.